

Beam Optics in the 1F Region to Support Isotope Production at the LERF

C. Tennant

Abstract

In this note we describe a reconfiguration of the 1F region in Jefferson Laboratory's Low Energy Recirculator Facility (LERF) in preparation for tests of radioisotope generation using high power electron beams. With the absence of two of the three cryomodules in the LERF linac, two additional triplets will be added to provide a robust optics solution for transporting relatively low energy beams (18.5 and 40.0 MeV). A dedicated isotope target beamline is being designed for the region immediately downstream of the energy recovery dump extraction chicane and will be covered in a separate note.

Introduction

The DOE recently approved project funding to test a novel way of generating radioisotopes using high energy electron beams. Specifically, the proposal aims to demonstrate useful yields of ^{67}Cu by photo-production using bremsstrahlung photons [1]. The experiment involves directing a low energy, high power electron beam onto a high-Z radiator to generate photons which are incident on a Gallium target. The target will then be sent off-site for radiochemical separation where the extraction efficiency and the yield of ^{67}Cu will be quantified.

Requirements

The crux of the proposal is the irradiation of a Gallium target with a high power electron beam in the Low Energy Recirculator Facility (LERF) at Jefferson Laboratory, removing the target and then chemically separating the ^{67}Cu offsite at VCU. There are two beam energies of interest, 18.5 and 40 MeV, delivering 1 kW of beam power for each. Additionally, a run at 40 MeV with 5 kW of beam power is planned. The beam parameters required for the experiment are summarized in Table 1.

Table 1: Beam parameters for the isotope production experiment.

Power (kW)	Energy (MeV)	Ave. Current (μA)
1	18.5	54
	40.0	25
5	40.0	125

Due to LCLS-II cryomodule testing in the LERF vault and the removal of 2 of the 3 cryomodules from the LERF, a re-design of the linac region is required. The solution must:

1. provide lossless transport of different energy beams to the isotope target
2. provide sufficient operational tunability
3. provide ease of setup

4. provide ease of verifying setup
5. keep the recirculation transport relatively intact
6. avoid unnecessary complexity, so as to maximize the budget available for beam operations

Though not a “must”, additionally we would like the solution to provide sufficient operational flexibility to perform experiments/measurements of interest to other users.

Lattice Solution

Before understanding the constraints and the present condition of the LERF vault, it is worthwhile to remember the nominal IR FEL Upgrade configuration and the nomenclature used. Figure 2 shows a schematic of the FEL layout with labels for the relevant regions and modules. The electron beam is generated and formed in a DC photocathode gun, accelerated in a quarter-cryomodule and merged onto the linac axis – all of which is denoted as the 0F region. The linac region which is comprised of three cryomodules and two intervening quadrupole triplets is the 1F region. The extraction chicane – which sends an energy recovered beam to the dump and the recirculating beam back onto the linac axis – marks the beginning of the 2F region (and which extends through the first recirculation arc which is not shown in the figure).

The LERF last ran in the fall of 2016 in support of the DarkLight experiment. Since that time the LERF vault has undergone significant change to accommodate testing LCLS-II cryomodules. The 0F region remains unchanged. The FEL cryomodules that were in Zone 2 and Zone 3 have been removed and the cryomodule that once occupied Zone 4 has been moved to Zone 2. The 2F region will be reworked slightly by adding a dipole after the extraction chicane to direct beam to a dedicated isotope beamline. The details of this design will be covered in a separate note. Here, we consider only modifications to the 1F region.

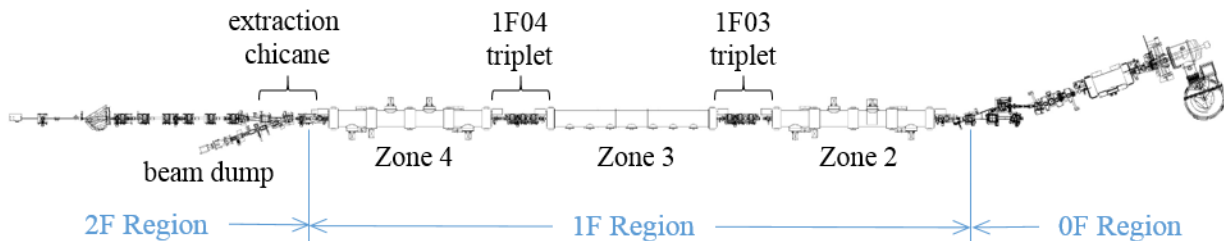


Figure 2: Schematic of the 0F, 1F and beginning of the 2F region in the nominal IR FEL Upgrade configuration. Beam is generated in the injector (0F region) and is transported from right to left in the figure.

The 1F03 triplet remains the same, leaving the region from the exit of the last quad in the triplet (QX1F03B) to the entrance of the first extraction chicane dipole (GV2F00) empty (roughly 20 m). The major constraint is the presence of a Helium transfer line for the LCLS-II testing which crosses the linac axis roughly where the 1F04 triplet once was. There is sufficient clearance for a beam pipe but not for beamline components. Figure 3 shows an accurate rendering of the current state of the 1F region.

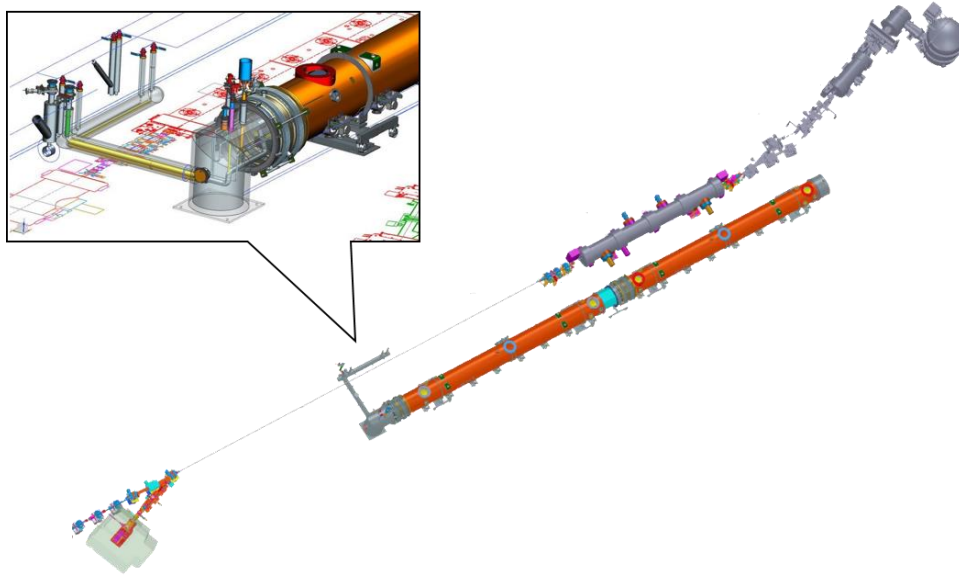


Figure 3: Rendering of the LERF vault with the LCLS-II cryomodules (orange) in place, parallel to the linac axis, along with the transfer line (inset) [2].

This is not the first time the LERF has been configured for low energy irradiation experiments. In 2011 the machine was setup to deliver 10 MeV beam to users in the straight ahead dump. For that experiment, beam was accelerated near crest through the first two cryomodules and then decelerated through the last cryomodule down to 10 MeV [3]. This offered the advantage that the beam was quickly accelerated and stayed at relatively high energy (compared to the injection energy) for much of the transport. With two of the cryomodules removed from the LERF this is not an option for the isotope production experiment. The priority is for a robust and operationally simple configuration.

The solution for the isotope production experiment (near term) – and as long as the cryomodules in zones 3 and 4 are missing (longer term) – is to install two additional quadrupole triplets in the 1F region, as suggested by A. Hutton [4]. Following the extraction chicane is a six quadrupole telescope. A dipole directing beam to the isotope beamline will be installed downstream of the third quadrupole (QX2F03). We therefore treat the first three quads (QX2F01-03) as a triplet. For symmetry and to simplify installation, the distance from the center quadrupole from one triplet to the next is identical (8.7151 m). Maintaining the same nomenclature as before, the first triplet downstream of 1F03 will be denoted as the 1F04 triplet and the one downstream of it will be denoted as the 1F05 triplet. The distance from the middle quadrupole of the 1F03 triplet to the middle quadrupole of the 1F04 triplet is the same as the distance from the middle quadrupole of the 1F04 triplet to the middle quadrupole of the 1F05 triplet which is the same as the distance from the middle quadrupole of the 1F05 triplet to the middle quadrupole of the 2F “triplet”. Figure 4 illustrates the layout differences in the 1F region between the nominal FEL configuration and the new configuration in the absence of cryomodules in zone 3 and 4. Figure 5 displays a plan view of the 1F region. Appendix A provides coordinates for the new layout.

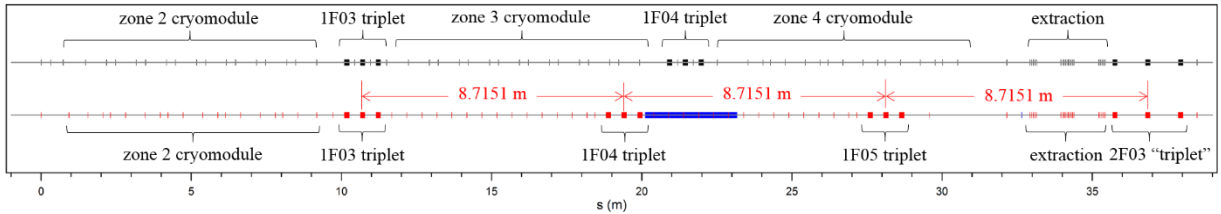


Figure 4: Placement of magnetic beamline components in the 1F region for the FEL (top) and with the new optics solution for isotope production (bottom). The blue section on the lower layout represents the location of the LCLS-II transfer line. (Beam direction is from left to right).



Figure 5: Plan view of the 1F region showing the placement of the two additional triplets. The LCLS-II transfer line is also shown for reference. (Beam direction is from left to right).

One of the challenges of generating an optics solution is the lack of experimentally measured Twiss parameters at the entrance of the linac (1F region). Due to space constraints in the 0F region, there is little opportunity to characterize the beam to the desired degree. For this exercise, it is assumed that the beam is symmetric and has beta functions of 5 m and alphas of 0 (neither diverging nor converging) at the entrance to the zone 2 cryomodule. This is a reasonable starting point based on previous operational experience.

An additional challenge is that the experimental program requires running at two different, relatively low, energy setpoints. Because of the low energy, transverse RF focusing in the cryomodule is significant and dependent on how the gradients are distributed amongst the 8 cavities. (To more clearly see the effect that gradient distribution has on transverse optics, see Appendix B). For 40.0 MeV the cryomodule will be running near the maximum achievable gradient in each cavity whereas for 18.5 MeV the gradients will be distributed among the first 4 cavities only (this is discussed more fully in the following section). The result is that the Twiss parameters at the exit of the cryomodule at 40.0 MeV (18.5 MeV) yield betas of 7.2 m (10.4 m) and alphas of -1.0 (-0.9). Each of the four triplets are run with the outboard pair of quadrupoles at the same strength. Figures 6 and 7 show the Twiss parameters for the solutions at 18.5 and 40.0 MeV, respectively. The beta functions are moderate and symmetric and lend themselves to quadrupole scans for both planes at multiple points (this is discussed in more detail in a later section). The additional triplets offer sufficient flexibility in tuning the beam optics (e.g. if measured Twiss parameters at the exit of the cryomodule differ substantially from the model) and provide knobs to fine tune the beam to meet specifications at the isotope target.

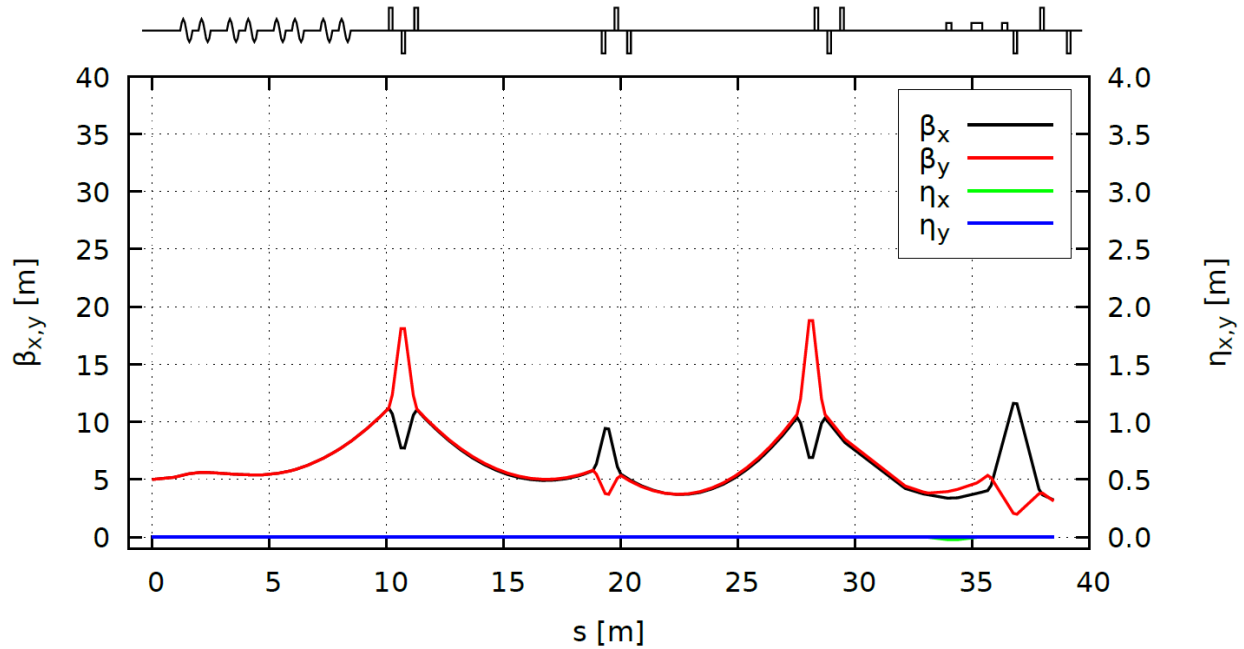


Figure 6: Twiss parameters for the optics solution in the 1F region for $E_{\text{final}} = 18.5$ MeV/c. Beam starts at the entrance to the cryomodule in zone 2 ($s = 0$ m) and extends to the exit of the QX2F03 quadrupole ($s = 39$ m).

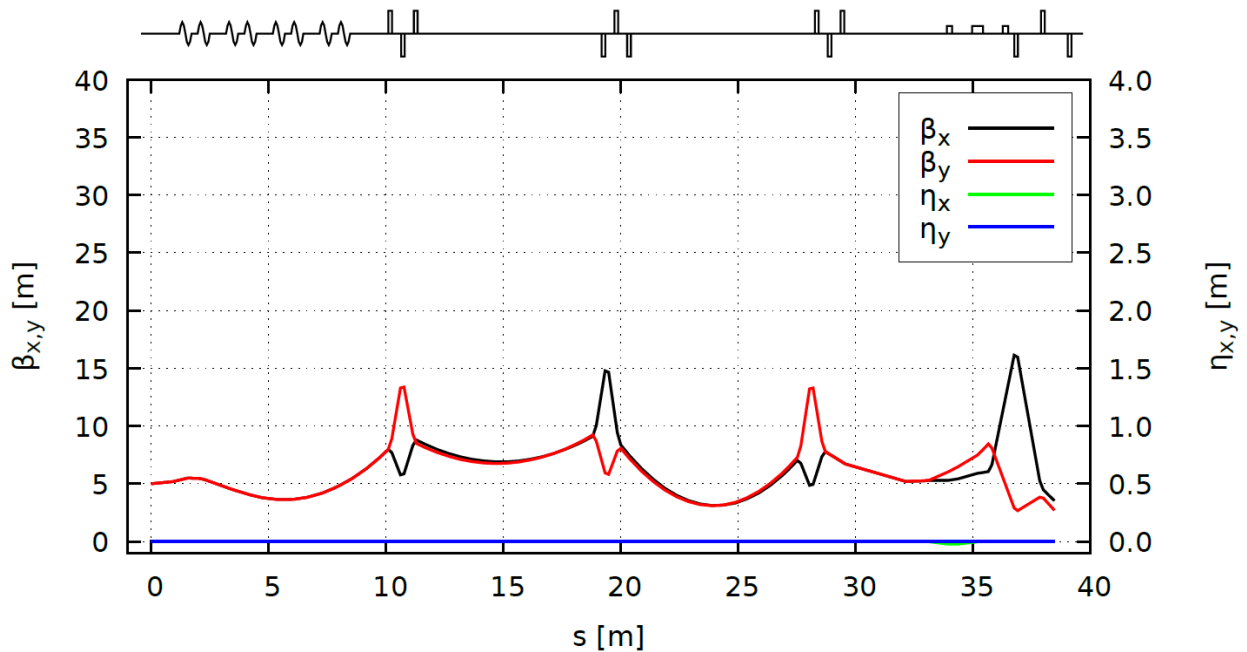


Figure 7: Twiss parameters for the optics solution in the 1F region for $E_{\text{final}} = 40.0$ MeV/c. Beam starts at the entrance to the cryomodule in zone 2 ($s = 0$ m) and extends to the exit of the QX2F03 quadrupole ($s = 39$ m).

The design quadrupole strengths for each energy are summarized in Table 2 and represent the starting point for beam operations.

Table 2: Quadrupole strengths for the quadrupoles in the 1F and beginning of the 2F region for two different energy setpoints. The quadrupoles are listed in the order that they are seen by the beam.

Quadrupole	Integrated Field (G)	
	18.5 MeV	40.0 MeV
QX1F03	300.83	650.45
QX1F03A	-571.12	-1234.85
QX1F03B	300.83	650.45
QX1F04	-324.90	-702.49
QX1F04A	610.92	1320.91
QX1F04B	-324.90	-702.49
QX1F05	350.82	758.52
QX1F05A	-654.43	-1414.98
QX1F05B	350.82	758.52
QX2F01	-347.12	-750.52
QX2F02	510.95	1104.76
QX2F03	-347.12	-750.52

Quadrupole Triplets

For ease of installation, the two additional triplets (1F04 and 1F05) will be identical to the 1F03 triplet, both in terms of their layout/spacing and in terms of their diagnostic packages. Figure 8 provides a sketch of the 1F03 triplet with the relevant quadrupole spacing and diagnostics.

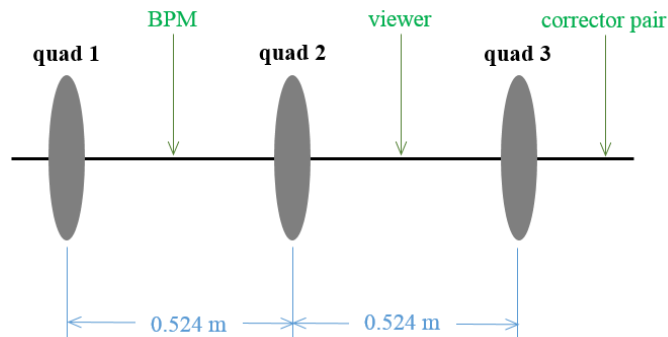


Figure 8: Layout of the 1F03 quadrupole triplet which provides a template for the 1F04 and 1F05 triplets. Beam direction is from left to right.

Operational Aspects

In this section we consider operational aspects of the modified optics solution in the 1F region of the LERF.

1. Nothing has changed in the 0F region and the injector will be set to provide 8 MeV/c electrons to the linac. This is a bit lower energy than nominal FEL operations, however, by lowering the energy we reduce field emission from the quarter cryouunit. It is also

the last configuration used for LERF operations and should, in principle, be easier to re-establish.

2. The cryomodule that now sits in Zone 2 is an older module with limited gradient capability. No longitudinal manipulations are required for the isotope experiments so beam will be accelerated on-crest. To reach 40 MeV, the module will need to provide an energy gain of 32 MV (or, 4 MV/cavity) which is the upper limit of what it can provide. For situations where the energy at the isotope target is less, the gradients should be front-end loaded. That is, to get the necessary (transverse) RF focusing the gradients should be distributed in the first 4 cavities with the last 4 cavities set to zero gradient and de-tuned. For example, to achieve 18.5 MeV, the module needs to provide 10.5 MV energy gain and the gradients should be distributed as: (3.0, 3.0, 3.0, 1.5, 0, 0, 0, 0) MV/cavity.
3. Once the usual beam threading and centering in quadrupoles is complete, it is important to establish the Twiss parameters at the exit of the cryomodule (as noted previously, we do not have the opportunity for quantitative beam measurements upstream). To that end, we will use the first quadrupole in the 1F03 triplet together with a downstream viewer to do a standard quad scan. Details of this measurement will be discussed in a separate section below.
4. Once the input Twiss parameters have been measured, the values will be entered into the model and we can virtually tune-up the machine optics. We use the program Bmad which is an open source code for simulating relativistic charged-particle dynamics developed at Cornell University in the 1990s [5]. One of its features is the ability to vary attributes of beamline components (e.g. quadrupole strengths) in an interactive way. (For those familiar with prior FEL operations, this is the analogue of D. Douglas' Excel spreadsheet for machine tuning [6]). A screenshot of the program showing the model beta functions in the 1F region (top), the quadrupole strengths that can be altered (middle) and layout (bottom) is given in Figure 9.
5. Performing a second quad scan using a downstream quadrupole – either the 1F04 or 1F05 triplet – will provide verification of the optics setup and benchmarking with the model.

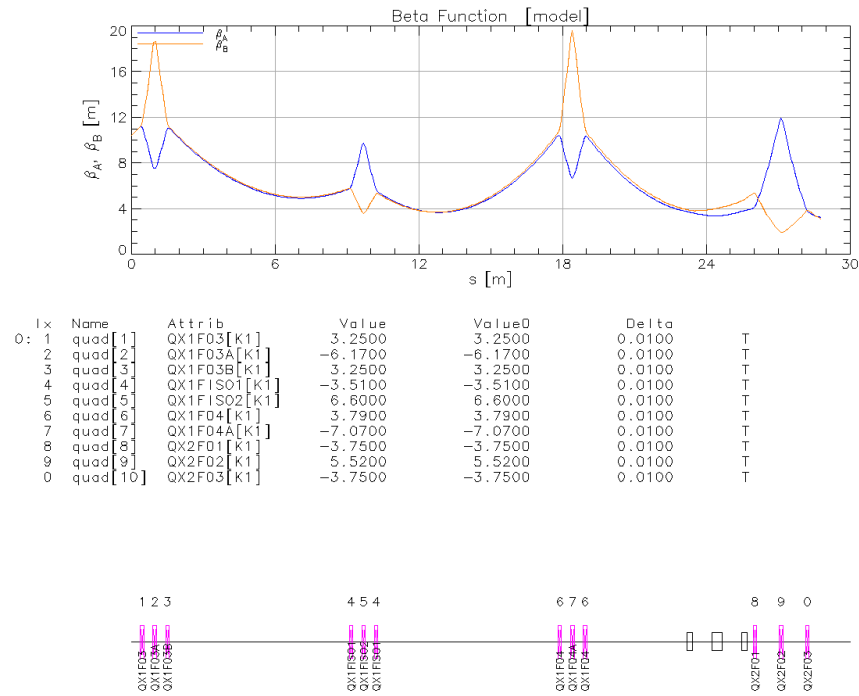


Figure 9: Screenshot from Bmad which gives users the ability to virtually tune the machine.

Beam Viewers

Functioning beam viewers are critical for the operation of the LERF. They serve more than a qualitative measurement (is the beam there or not?) but are the primary beam diagnostic for a variety of beam-based measurements. For nominal energy-recovered FEL operations, the linac viewers either had holes in the view screens to allow the first pass beam through and then to be able to image the second pass beam, or were made of a mesh-type material to allow both beams to be imaged simultaneously. The isotope experiment does not need this functionality, however it does require the beam to be imaged at energies lower than usual. The requirements on the proposed five viewers in the 1F region (one at each of the three triplets, one on fast valve girder immediately downstream of the 1F03 triplet and the LDRD viewer downstream of the 1F05 triplet) are that they:

1. Need to work at low energy. Therefore all view screens should be replaced with YAG crystals. Note that these are a long lead time item (10 weeks) [7].
2. Need to image well. This means there is sufficient signal to make quantitative measurements or appropriate neutral density filters installed in the event that there is too much signal.
3. Need to be calibrated. In order to get quantitative information, namely the beam size, the view screens need to be calibrated so the imaging software can convert sizes from units of pixels to units of length. One way to do this is to put well-defined markings on the view screen which can then be correlated to pixels in the imaging software.
4. Need to be aligned. To avoid unnecessary downtime and machine accesses, viewers should be aligned.

Quadrupole Scan

The importance of being able to do a quadrupole scan cannot be overstated. In addition to providing vital beam quality metrics (transverse emittances) it also yields necessary input for the model to tune up the optics. Though in principle the measurement is straightforward, there are several challenges that exist (for a detailed analysis of the DarkLight quadrupole scan data and a discussion of the challenges, see Ref. [8]):

1. One of the vital aspects of beam operations is the link between the viewer and the beam operators. In the LERF we utilize the Beamanizer – a powerful piece of software created in LabView which digitizes and displays images from viewers [9]. In addition to displaying images, it also computes real-time statistics of user-defined regions of the image as well as providing curve fitting features of image projections in each plane (horizontal and vertical). However, as the subject matter expert for the software is no longer employed at the laboratory, there have been struggles to get it working optimally. Prior to DarkLight, much work was required to make the software compatible with Windows 7 and now, 2 years later, additional work is required to make it compatible with Windows 10 [10]. Some of the key features – like the real-time statistics of a user-defined region on the viewer – were not functioning. This means that a simple quadrupole scan required dedicated off-line analysis to extract beam size information and to extract emittances and Twiss parameters.
2. Note that the LERF does not have a standard, automated way to take and analyze quadrupole scan data. Over the years, individuals have resorted to whatever methods they feel most comfortable with (i.e. using Beamanizer, Excel, elegant, etc.).

By way of example, Figure 10 shows the results of a simulated measurement by scanning quadrupole QX1F03B (the last quad in the 1F03 triplet) and using the downstream viewer embedded in the 1F04 triplet (all 1F04 quads are turned off). Because of the symmetry of the beam optics and the fact that there is a beam waist at the viewer, both transverse planes can be scanned simultaneously. A similar scan can be achieved by scanning a quadrupole in the 1F04 triplet and using the downstream viewer in the 1F05 triplet. This provides multiple points at which we can benchmark with model optics and make adjustments if necessary.

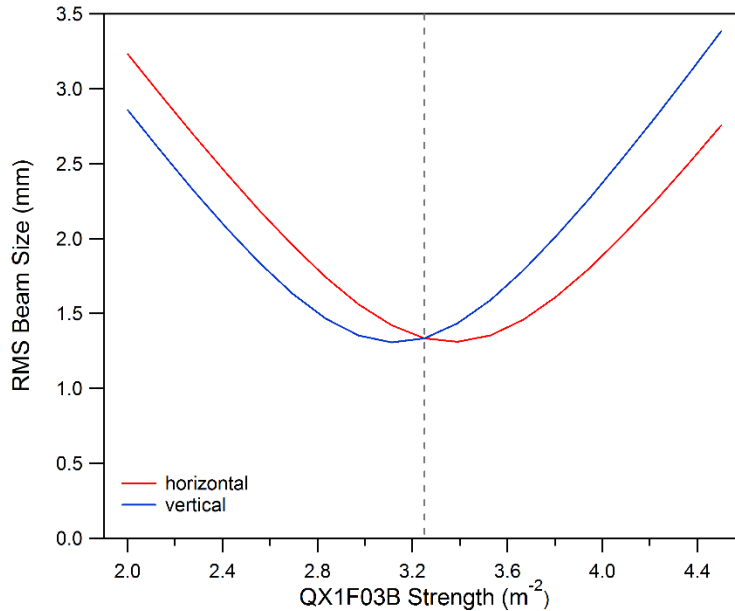


Figure 10: Simulated quadrupole scan using the QX1F03B quadrupole and the downstream viewer in the 1F04 triplet. The dashed vertical line represents the quadrupole strength for the nominal optics setup.

Summary

We have described a proposed modification of the 1F region in the LERF to support the isotope production experiment. The three quadrupole triplets (1F03, 1F04 and 1F05) provide a robust solution for transporting high power (order 1 to 5 kW), low energy beams. The region is sufficiently instrumented with beam diagnostics – in particular five beam viewers – so as to characterize the beam via quadrupole scans and make appropriate adjustments to match the lattice. A forthcoming note will address the design of the 2F region and specifically the dedicated isotope beamline.

References

- [1] A. Hutton, D. Wells and J. Zweit, “Isotope Production R&D at Jefferson Lab’s High-Power Electron Accelerators”, Proposal in Response to DOE National Lab Announcement LAB 16-1588.
- [2] figure courtesy J. Gubeli.
- [3] see, for example, All-Saves from March 16, 2011.
- [4] A. Hutton, *private communication*.
- [5] D. Sagan, “Bmad: A Relativistic Charged Particle Simulation Library”, Nucl. Instrum. Methods Phys. Res., Sect. A 558, 356 (2006).
- [6] D. Douglas et al., “Simplified Charged Particle Beam Transport Modeling Using Commonly Available Commercial Software”, Proceedings of 2007 Particle Accelerator Conference, Albuquerque, NM, pp. 3651-3653 (2007).
- [7] J. Gubeli, *private communication*.

- [8] C. Tennant, “Analysis of the Quadrupole Scan Method to Measure Emittance in the LERF Using the Beamanizer”, Jefferson Laboratory Technical Note 16-047 (2016).
- [9] The Beamanizer was developed by Pavel Evtushenko.
- [10] B. Freeman, “LERF Resuscitation” meeting, August 30, 2018.
- [11] K. Tremblay, Data Transmittal #F1885, September 18, 2018.

Appendix A: Hardware Layout

Figure A1 gives a plan view of the 1F region and distances between beamline components. Note that the distance between the magnetic centers of GV0F06A and GV2F00 given (33.6220 m) is based on the ideal coordinates reported from the Survey & Alignment group [11] and is 4.5 mm shorter than the model (i.e. the coordinates as given below in Table A1). The source of the discrepancy has not yet been determined, but as these two dipoles have not and will not be moved, the difference is not important.

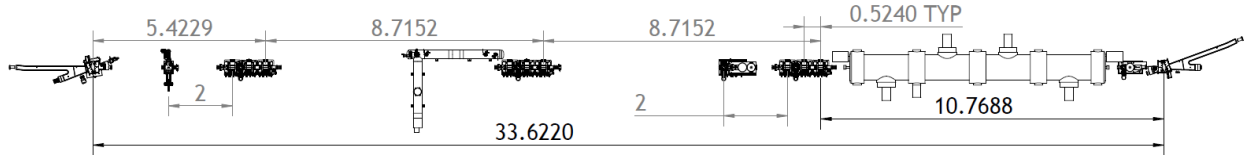


Figure A1: Labeled plan view of the 1F region with beamline components (note, all distances are in meters) [2].

Table A1 gives the hardware coordinates starting from the exit of the last injection merger dipole (GV0F06B) to the just upstream of the first extraction chicane dipole. Element names with a “-C” denote the coordinates of the center point of the element. (Drift lengths are split into multiple shorter sections to better resolve plots of the Twiss parameters).

Table A1: Hardware coordinates for the LERF 1F region.

Element	Element Type	X	Y	Z	Theta	Phi	Psi
		{m}	{m}	{m}	{rad}	{rad}	{rad}
BEG	MARK	0.04	0.00	0.0000	-0.35	0.00	0.00
GV0F06A-C	SBEN	0.02	0.00	0.1026	-0.17	0.00	0.00
GV0F06A	SBEN	0.00	0.00	0.2052	0.00	0.00	0.00
GV0F06A-VP	VERTEX-POINT	0.00	0.00	0.0994	-0.35	0.00	0.00
D1F01A	DRIF	0.00	0.00	0.6948	0.00	0.00	0.00
ORIGIN	WATCH	0.00	0.00	0.6948	0.00	0.00	0.00
D0	DRIF	0.00	0.00	1.6224	0.00	0.00	0.00
DA1	DRIF	0.00	0.00	2.2562	0.00	0.00	0.00
R428	RFCA	0.00	0.00	2.7569	0.00	0.00	0.00
DA2	DRIF	0.00	0.00	3.0062	0.00	0.00	0.00
R427	RFCA	0.00	0.00	3.5069	0.00	0.00	0.00
DA3	DRIF	0.00	0.00	4.1668	0.00	0.00	0.00
R426	RFCA	0.00	0.00	4.6675	0.00	0.00	0.00
DA2	DRIF	0.00	0.00	4.9168	0.00	0.00	0.00
R425	RFCA	0.00	0.00	5.4175	0.00	0.00	0.00
DA3	DRIF	0.00	0.00	6.0774	0.00	0.00	0.00
R424	RFCA	0.00	0.00	6.5781	0.00	0.00	0.00
DA2	DRIF	0.00	0.00	6.8274	0.00	0.00	0.00
R423	RFCA	0.00	0.00	7.3281	0.00	0.00	0.00
DA3	DRIF	0.00	0.00	7.9880	0.00	0.00	0.00
R422	RFCA	0.00	0.00	8.4887	0.00	0.00	0.00
DA2	DRIF	0.00	0.00	8.7380	0.00	0.00	0.00

R421	RFCA	0.00	0.00	9.2387	0.00	0.00	0.00
DA1	DRIF	0.00	0.00	9.8724	0.00	0.00	0.00
DGAP	DRIF	0.00	0.00	10.4172	0.00	0.00	0.00
DG1	DRIF	0.00	0.00	10.7958	0.00	0.00	0.00
QX1F03-C	QUAD	0.00	0.00	10.8708	0.00	0.00	0.00
QX1F03	QUAD	0.00	0.00	10.9458	0.00	0.00	0.00
DG2	DRIF	0.00	0.00	11.3198	0.00	0.00	0.00
QX1F03A-C	QUAD	0.00	0.00	11.3948	0.00	0.00	0.00
QX1F03A	QUAD	0.00	0.00	11.4698	0.00	0.00	0.00
DG2	DRIF	0.00	0.00	11.8438	0.00	0.00	0.00
QX1F03B-C	QUAD	0.00	0.00	11.9188	0.00	0.00	0.00
QX1F03B	QUAD	0.00	0.00	11.9938	0.00	0.00	0.00
DG3	DRIF	0.00	0.00	12.3724	0.00	0.00	0.00
FIT1	MARK	0.00	0.00	12.3724	0.00	0.00	0.00
DAA	DRIF	0.00	0.00	12.8724	0.00	0.00	0.00
DAA	DRIF	0.00	0.00	13.3724	0.00	0.00	0.00
DAA	DRIF	0.00	0.00	13.8724	0.00	0.00	0.00
DAA	DRIF	0.00	0.00	14.3724	0.00	0.00	0.00
DAA	DRIF	0.00	0.00	14.8724	0.00	0.00	0.00
DAA	DRIF	0.00	0.00	15.3724	0.00	0.00	0.00
DAA	DRIF	0.00	0.00	15.8724	0.00	0.00	0.00
DAA	DRIF	0.00	0.00	16.3724	0.00	0.00	0.00
DAA	DRIF	0.00	0.00	16.8724	0.00	0.00	0.00
DAA	DRIF	0.00	0.00	17.3724	0.00	0.00	0.00
DAA	DRIF	0.00	0.00	17.8724	0.00	0.00	0.00
DAA	DRIF	0.00	0.00	18.3724	0.00	0.00	0.00
DAA	DRIF	0.00	0.00	18.8724	0.00	0.00	0.00
DAB	DRIF	0.00	0.00	19.1324	0.00	0.00	0.00
DG1	DRIF	0.00	0.00	19.5110	0.00	0.00	0.00
QX1F04-C	QUAD	0.00	0.00	19.5860	0.00	0.00	0.00
QX1F04	QUAD	0.00	0.00	19.6610	0.00	0.00	0.00
DG2	DRIF	0.00	0.00	20.0350	0.00	0.00	0.00
QX1F04A-C	QUAD	0.00	0.00	20.1100	0.00	0.00	0.00
QX1F04A	QUAD	0.00	0.00	20.1850	0.00	0.00	0.00
DG2	DRIF	0.00	0.00	20.5590	0.00	0.00	0.00
QX1F04B-C	QUAD	0.00	0.00	20.6340	0.00	0.00	0.00
QX1F04B	QUAD	0.00	0.00	20.7090	0.00	0.00	0.00
DG3	DRIF	0.00	0.00	21.0876	0.00	0.00	0.00
FIT2	MARK	0.00	0.00	21.0876	0.00	0.00	0.00
DAA	DRIF	0.00	0.00	21.5876	0.00	0.00	0.00
DAA	DRIF	0.00	0.00	22.0876	0.00	0.00	0.00
DAA	DRIF	0.00	0.00	22.5876	0.00	0.00	0.00
DAA	DRIF	0.00	0.00	23.0876	0.00	0.00	0.00
DAA	DRIF	0.00	0.00	23.5876	0.00	0.00	0.00
DAA	DRIF	0.00	0.00	24.0876	0.00	0.00	0.00
DAA	DRIF	0.00	0.00	24.5876	0.00	0.00	0.00
DAA	DRIF	0.00	0.00	25.0876	0.00	0.00	0.00
DAA	DRIF	0.00	0.00	25.5876	0.00	0.00	0.00

DAA	DRIF	0.00	0.00	26.0876	0.00	0.00	0.00
DAA	DRIF	0.00	0.00	26.5876	0.00	0.00	0.00
DAA	DRIF	0.00	0.00	27.0876	0.00	0.00	0.00
DAA	DRIF	0.00	0.00	27.5876	0.00	0.00	0.00
DAB	DRIF	0.00	0.00	27.8476	0.00	0.00	0.00
DG3	DRIF	0.00	0.00	28.2262	0.00	0.00	0.00
QX1F05-C	QUAD	0.00	0.00	28.3012	0.00	0.00	0.00
QX1F05	QUAD	0.00	0.00	28.3762	0.00	0.00	0.00
DF2	DRIF	0.00	0.00	28.7502	0.00	0.00	0.00
QX1F05A-C	QUAD	0.00	0.00	28.8252	0.00	0.00	0.00
QX1F05A	QUAD	0.00	0.00	28.9002	0.00	0.00	0.00
DF2	DRIF	0.00	0.00	29.2742	0.00	0.00	0.00
QX1F05B-C	QUAD	0.00	0.00	29.3492	0.00	0.00	0.00
QX1F05B	QUAD	0.00	0.00	29.4242	0.00	0.00	0.00
DF1	DRIF	0.00	0.00	30.2752	0.00	0.00	0.00
FIT3	MARK	0.00	0.00	30.2752	0.00	0.00	0.00
D2EXTRA	DRIF	0.00	0.00	32.8448	0.00	0.00	0.00
DBCM	DRIF	0.00	0.00	33.6204	0.00	0.00	0.00
GV2F00-C	SBEN	0.00	0.00	33.7291	0.01	0.00	0.00
GV2F00	SBEN	0.00	0.00	33.8378	0.02	0.00	0.00
GV2F00-VP	VERTEX-POINT	0.00	0.00	33.7291	0.00	0.00	0.00
DREINJ1	DRIF	0.02	0.00	34.6530	0.02	0.00	0.00
GU2F00-C	SBEN	0.02	0.00	34.8704	0.00	0.00	0.00
GU2F00	SBEN	0.02	0.00	35.0878	-0.02	0.00	0.00
GU2F00-VP	VERTEX-POINT	0.03	0.00	34.8704	0.02	0.00	0.00
DREINJ1	DRIF	0.00	0.00	35.9030	-0.02	0.00	0.00
GV2F00A-C	SBEN	0.00	0.00	36.0117	-0.01	0.00	0.00
GV2F00A	SBEN	0.00	0.00	36.1204	0.00	0.00	0.00
FIT4	MARK	0.00	0.00	36.1204	0.00	0.00	0.00
GV2F00A-VP	VERTEX-POINT	0.00	0.00	36.0117	-0.02	0.00	0.00
DM11ALT	DRIF	0.00	0.00	36.3704	0.00	0.00	0.00

Appendix B: Effect of Gradient Distribution on Transverse Optics

Figure B1 plots the transverse beta function through a cryomodule which is set to give the same output energy (18 MeV) but with the gradients distributed in various ways. For example, the red and blue trace show the difference when the energy gain occurs in the first four versus the last four cavities, respectively. The plot illustrates the importance of RF focusing, particularly at low energies.

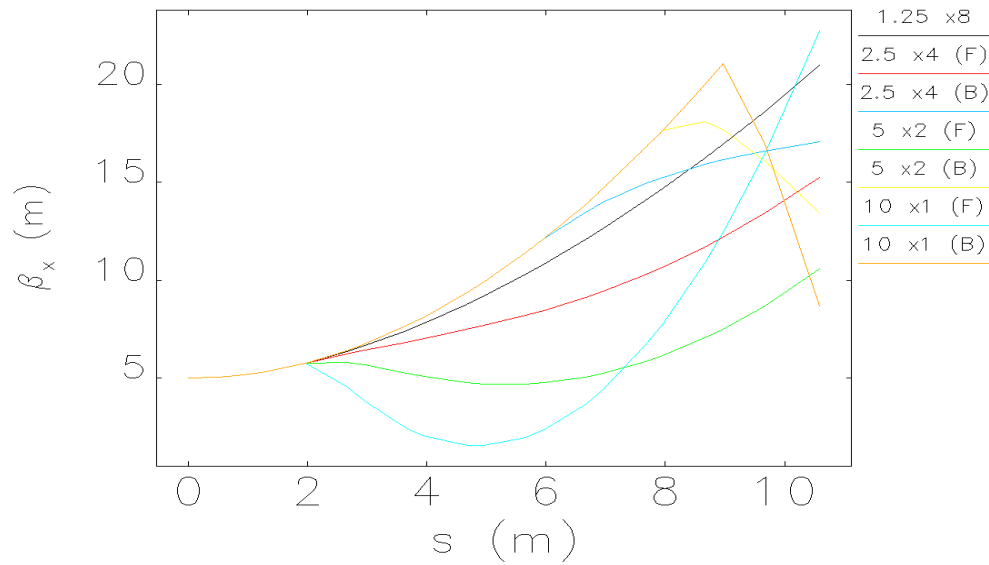


Figure B1: Plot of horizontal beta functions through a cryomodule with a fixed total energy gain (10 MV) but with various distributions of gradient among the 8 cavities.